Inclusion Complexation of Diquat and Paraquat by the Hosts Cucurbit[7]uril and Cucurbit[8]uril

Yonghua Ling,[a] Joel T. Mague,[b] and Angel E. Kaifer*[a]

Abstract: The binding interactions in aqueous solution between the dicationic guest diquat (DQ^{2+}) and the cucurbit[7]uril (CB7) and cucurbit[8]uril (CB8) hosts were investigated by ^1H NMR, UV/Vis, and fluorescence spectroscopy; mass spectrometry; single-crystal X-ray diffraction; and electrochemical techniques. The binding data were compared with previously reported results for the related paraquat guest (PQ^{2+}). DQ^{2+} was found to bind poorly ($K = 350\,\text{M}^{-1}$) inside CB7 and more effectively ($K = 4.8 \times 10^4\,\text{M}^{-1}$) inside CB8. One-electron reduction led to increased binding affinity with both hosts ($K_r = 1 \times 10^4\,\text{M}^{-1}$ with CB7 and $K_r = 6 \times 10^5\,\text{M}^{-1}$ for CB8). While ^1H NMR spectroscopic data revealed that DQ^{2+} is not fully included by CB7, the crystal structure of the $CB8 \cdot DQ^{2+}$ complex—obtained from single-crystal X-ray diffraction—clearly establishes its inclusion nature. Overall, both diquat and its one-electron reduced radical cation are bound more effectively by CB8 than by CB7. In contrast to this, paraquat exhibits selectivity for CB7, but its radical cation forms a highly stable dimer inside CB8. These differences highlight the pronounced sensitivity of cucurbit[n]uril hosts to guest features such as charge, charge distribution and shape.

Keywords: cyclic voltammetry · electrochemistry · host–guest systems · inclusion compounds · supramolecular chemistry

Introduction

Diquat (DQ^{2+}) and paraquat (PQ^{2+}) are nonselective contact herbicides with a strong ability to engage in electron-transfer reactions and, thus, disrupt natural electron-transport chains crucial to the survival of biological systems.[1] Both species are divalent cations, with a pronounced electron-deficient character, that undergo two consecutive, one-electron reductions according to the general scheme given in Equations (1) and (2).

$$Q^{2+} + e^- \rightleftharpoons Q^{\cdot+} \qquad E_1^o \qquad (1)$$

$$Q^{\cdot+} + e^- \rightleftharpoons Q \qquad E_2^o \qquad (2)$$
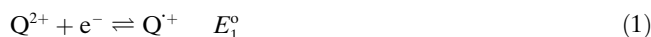
Both reduction processes are electrochemically reversible (kinetically fast) and take place at accessible potentials in aqueous and nonaqueous solutions. In aqueous media, reduction removes positive charge from the structures, often leading to fairly hydrophobic radical cation ($Q^{\cdot+}$) and neutral species (Q), which may precipitate on the working electrode surface and give rise to strong distortions in the shape of the voltammetric peaks.

The cucurbit[n]urils are macrocyclic hosts formed by the acid condensation of glycoluril in the presence of formaldehyde.[2,3] The initial isolation by Kim and co-workers[4] of cucurbit[n]urils with $n > 6$ has led to intense research activity on the binding properties of these hosts. Cucurbit[7]uril (CB7) and cucurbit[8]uril (CB8) have been the subject of particular attention. Kim's group[5] and our own[6] reported

[a] Y. Ling, Prof. Dr. A. E. Kaifer
Center for Supramolecular Science and Department of Chemistry
University of Miami, Coral Gables, FL 33124–0431 (USA)
Fax: (+1)305-284-4571
E-mail: akaifer@miami.edu

[b] Prof. Dr. J. T. Mague
Department of Chemistry, Tulane University
New Orleans, LA 70118 (USA)

Supporting information for this article is available on the WWW under http://www.chemeurj.org/ or from the author.
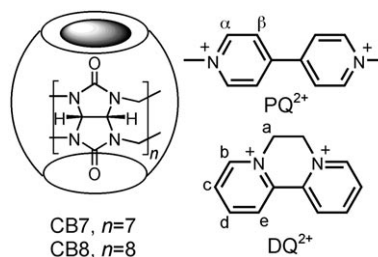
in 2002 that paraquat forms a highly stable inclusion complex with CB7. Kim and co-workers also reported the formation of a 1:1 inclusion complex between paraquat and CB8.[7] Upon one-electron reduction of paraquat, CB8 was also found to enhance the formation of the radical cation dimer $(PQ^{•+})_2$, which is strongly stabilized in the inclusion complex $CB8 \cdot (PQ^{•+})_2$.[7] Furthermore, CB8 forms highly stable ternary complexes, in which PQ^{2+} and a suitable aromatic electron donor are included in its cavity.[8] Kim et al. have taken advantage of these binding interactions to design and prepare various switchable molecular systems.[9–15] Our own group has utilized CB8 for the redox control of self-assembly[16] and size selection[17] with dendronized viologens and aromatic electron donors.

The two quaternized nitrogen atoms in paraquat are separated by a distance of ca. 9.5 Å, which is only slightly longer than the distance (9.1 Å) between the two carbonyl oxygen rims on the cavity openings of the cucurbiturils. The similarity between these two distances is crucial for the development of strong ion–dipole interactions between the quaternized nitrogen atoms on the included guest and the corresponding carbonyl oxygen rims on the host. We have investigated other dicationic species with a similar separation distance between their two quaternized nitrogen atoms. Specifically, we have shown that 2,7-dimethyl-diazapyrenium[18] and 2,7-dimethyl-diazaphenanthrenium[19] are excellent guests for inclusion complexation by CB7 and CB8. The fluorescence properties of these compounds add an interesting analytical dimension to the binding interactions of their CB8 inclusion complexes with biologically relevant, aromatic electron donors, such as catechol,[20] indole[19] and their derivatives (tyrosine, dopamine, serotonin and tryptophan).

In this work, we report on the inclusion complexation between the hosts CB7 and CB8 and diquat as the guest, and compare its binding behavior with that exhibited by paraquat with the same hosts. The much shorter distance between the quaternized nitrogen atoms in diquat has a strong effect on its binding behavior and illustrates the structural and charge distribution requirements needed to optimize, in general, the binding affinity between any guest and the cucurbit[*n*]uril hosts.

Results and Discussion

The interaction of diquat with CB7 was initially investigated using ^{1}H NMR spectroscopy. Figure 1 shows the effect that CB7 has on the chemical shift of the aromatic protons of DQ^{2+} in a 0.1 M solution of NaCl in D_2O. All the aromatic protons experience gradual upfield displacements as the concentration of CB7 increases. The CB7-induced shifts continue after the concentrations of CB7 surpass one equivalent, suggesting that the corresponding equilibrium association constant (*K*) has a moderate value. While all the aromatic protons of the guest are sensitive to the presence of CB7, the protons adjacent to the quaternized nitrogen (b, see Figure 1 for proton labels) show the largest complexa-
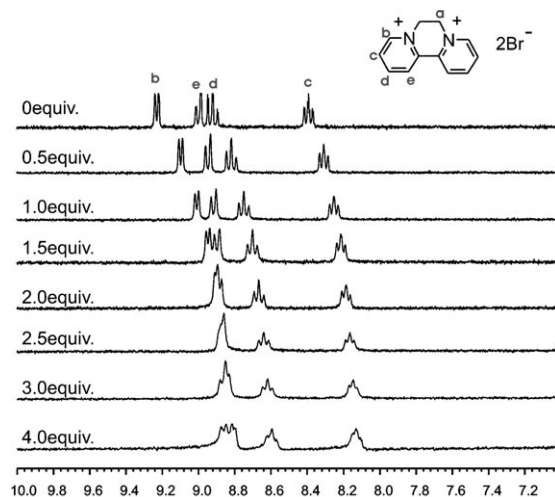

Figure 1. Partial ^{1}H NMR spectra (300 MHz, 0.1 M NaCl/D_2O) showing the aromatic protons of guest DQ^{2+} in the presence of increasing concentrations of CB7 host (indicated by the number of equivalents on each spectrum). Top spectrum obtained in the absence of CB7.

tion-induced shifts. We used the dependence of the chemical shift of these protons on the host concentration to determine the *K* value for the $CB7 \cdot DQ^{2+}$ complex and obtained a value of $340 \pm 40 \, M^{-1}$ in 0.1 M phosphate buffer (pH 7), by fitting the chemical shift values to a simple 1:1 binding isotherm (see plot in the Supporting Information). The relatively low binding affinity for this complex is in sharp contrast with the much larger value measured for the $CB7 \cdot PQ^{2+}$ complex ($1.2 \times 10^5 \, M^{-1}$ in the same medium). The importance of the ionic composition of the solution on the equilibrium association constants involving cucurbituril hosts cannot be overestimated.[21] Therefore, meaningful comparison can only be done when the medium compositions are similar.

What type of complex is formed between DQ^{2+} and CB7? An important observation in this regard is that the chemical shift of the guest's ethylene-bridge protons (a) is not affected by the interaction with CB7 (see the Supporting Information), a clear indication that these protons are not included inside the host's cavity. Furthermore, the kinetic lability of the $CB7 \cdot DQ^{•2+}$ complex (in fast exchange with the free guest in the NMR time scale) suggests a rather shallow mode of interaction, since full inclusion inside the cavity of cucurbit[7]uril often results in slow exchange between the free and bound guest on the NMR timescale.[6,18] We thus propose that the CB7 host partially includes one of the aromatic rings of DQ^{2+}, generating some favorable ion–dipole interactions between the carbonyl oxygen atoms on the including portal and the adjacent quaternized nitrogen on the guest. However, this shallow binding mode allows fast exchange of the host between the two aromatic rings of the guest, and results in a relatively weak complex. This binding mode is also consistent with the results of molecular modeling computations (see the Supporting Information).

The guest DQ^{2+} is also weakly fluorescent[22] and we took advantage of this spectroscopic property to analyze its binding to CB7 with a second analytical technique. In 0.1 M phos-

phate buffer (pH 7), increasing concentrations of the host lead to both a gradual enhancement of the fluorescent intensity emitted by DQ^{2+} and a clear bathochromic shift of its emission band maximum (from 347 to 365 nm, see Figure 2). These spectral changes are consistent with the
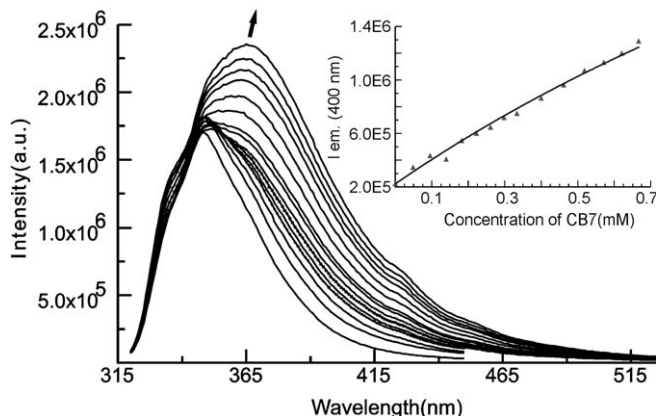

Figure 2. Dependence of the fluorescence intensity emitted by guest DQ^{2+} (17.7 μM) on the concentration of CB7 host (0–0.67 mM). The excitation intensity was 310 nm. The inset shows the best fit of the data to a 1:1 binding isotherm, which yields a K value of $350\,M^{-1}$.

host providing a less polar microenvironment for the guest, decreasing the number of possible nonradiative pathways available for deactivation of the excited state. A plot of the emission intensity (at 400 nm) as a function of CB7 concentration can be fitted to a 1:1 binding isotherm from which a K value of $350\pm45\,M^{-1}$ is derived. This value is in excellent agreement with the binding constant obtained from NMR spectroscopic data.

The reversible voltammetric behavior of DQ^{2+} affords another experimental technique to investigate its interactions with CB7. Figure 3 illustrates the cyclic voltammetric behavior of DQ^{2+} in the presence of various concentrations of CB7. In general terms, the addition of the host shifts the half-wave potential ($E_{1/2}$) for the first reduction process
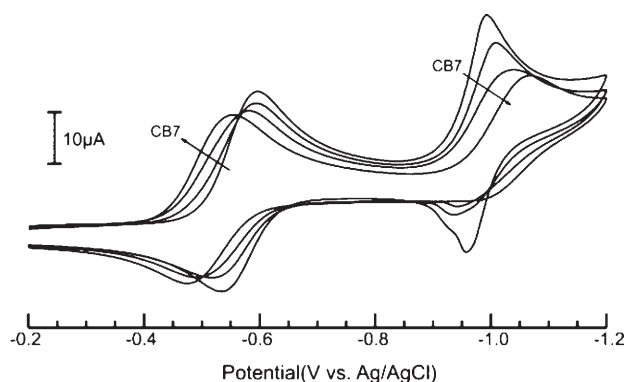

Figure 3. Cyclic voltammetric response on a glassy carbon working electrode (0.071 cm²) of solutions containing 1.29 mM DQ^{2+} in the presence of 0, 0.5, 1.0 and 2.0 equivalents of CB7. Medium: pH 7 0.1 M phosphate buffer. Scan rate: 0.1 V s^{-1}.

($DQ^{2+}/DQ^{\bullet+}$) to less negative values, while the second reduction process ($DQ^{\bullet+}/DQ$) shifts to more negative potentials. The observed behavior is consistent with the one-electron reduced guest ($DQ^{\bullet+}$) forming a more stable complex with CB7 than DQ^{2+}.[23] The moderate reduction in the overall current levels associated with the $DQ^{2+}/DQ^{\bullet+}$ wave is in agreement with the modest binding constant values determined for the $CB7\cdot DQ^{2+}$ complex from ^{1}H NMR and emission spectroscopic data. To further understand the electrochemical behavior of the $DQ^{2+}/DQ^{\bullet+}$ redox couple in the presence of the CB7 host, we fitted our experimental current–potential curves to digital simulations obtained using the Digi-Elch software package.[24–29] Since the $CB7\cdot DQ^{2+}$ complex shows modest stability, we assumed that the heterogeneous electron-transfer reaction takes place between the unbound DQ^{2+} and $DQ^{\bullet+}$ guests, and did not consider direct electron transfer between the corresponding CB7 complexes. This choice was justified by the mechanistic knowledge of heterogeneous electron-transfer reactions involving ferrocene[30,31] and cobaltocenium[32] derivatives in the presence of cyclodextrin hosts. In spite of the fact that these cyclodextrin complexes exhibit binding affinities slightly larger than that of the $CB7\cdot DQ^{\bullet2+}$ complex, their electrochemical reactions are thought to involve the free guests, not the inclusion complexes. Therefore, a similar mechanistic choice (see Scheme 1) appears to be jus-
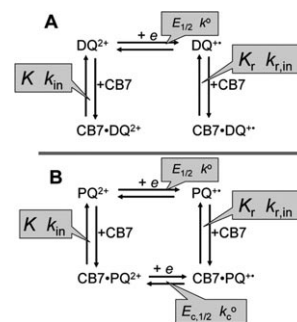
Scheme 1. Electrochemical and chemical reactions involved in the one-electron reduction of A) DQ^{2+} and B) PQ^{2+} in the presence of host CB7. The callouts contain the symbols assigned to the relevant parameters for each of the reactions.

tified for the $DQ^{2+}/DQ^{\bullet+}$ redox couple in the presence of CB7. Furthermore, this mechanism leads to reasonable diffusion coefficients for the complex species $CB7\cdot DQ^{2+}$ and $CB7\cdot DQ^{\bullet+}$, while the selection of a mechanism including direct electron transfer between the inclusion complexes forces the use of unrealistically high diffusion coefficients for these species in order to fit the experimental current levels. In stark contrast to this, the reduction of paraquat in the presence of CB7 is best rationalized by considering direct electron transfer between the inclusion complexes (Scheme 1), which highlights again their stability, considerably higher than that determined here for the corresponding diquat complexes.

Our digital simulations of the voltammetric current–potential curves were carried out using a series of reasonable assumptions based on well-established experimental observations. For instance, the standard rate constant (k^o) for the heterogenous electron transfer between DQ^{2+} and $DQ^{\bullet+}$ was assumed to be rather large ($k^o \geq 0.1\ cm\,s^{-1}$) and the corresponding charge-transfer coefficient (α) equal to $\frac{1}{2}$, since the observed electrochemical behavior is reversible in the surveyed range of scan rates. Similar assumptions were made for the $PQ^{2+}/PQ^{\bullet+}$ and $CB7\cdot PQ^{2+}/CB7\cdot PQ^{\bullet+}$ redox couples, in accordance with the reversible electrochemical behavior observed in all these cases. The diffusion coefficients were estimated by pulse gradient stimulated echo (PGSE) NMR techniques[33] and the kinetic rate constants for association of the CB7 complexes were also assumed to be relatively fast in all cases (we took $k_{in} = 1 \times 10^9\ M^{-1}\,s^{-1}$), since we did not observe voltammetric behavior suggesting slow association kinetics. The diffusion coefficient for free CB7 was found to be $3.14 \times 10^{-6}\ cm^2\,s^{-1}$ from PGSE NMR techniques. This is an important value and it acts as a reference for the expected values of the complexes investigated here. Clearly it is reasonable to anticipate that the complexes should have diffusion coefficients lower or slightly lower than the value observed for the free host.

Table 1 collects the parameters used as input data for the fitting of the digital simulations to the cyclic voltammetric data for both diquat and paraquat. Figures 4 and 5 show the

Table 1. Electrochemical, thermodynamic, kinetic and diffusion parameters (at 25°C) used to optimize the fitting of the digital simulations.

Diquat	Paraquat
$DQ^{2+} + e^- = DQ^{\bullet+}$	$PQ^{2+} + e^- = PQ^{\bullet+}$
$E_{1/2} = -0.57\ V$	$E_{1/2} = -0.65\ V$
$k^o = 0.1\ cm\,s^{-1}\ (\alpha = 0.5)$	$k^o = 0.1\ cm\,s^{-1}\ (\alpha = 0.5)$
$D_{DQ^{2+}} = D_{DQ^+} = 6.7 \times 10^{-6}\ cm^2\,s$	$D_{PQ^{2+}} = D_{PQ^+} = 6.7 \times 10^{-6}\ cm^2\,s$
$DQ^{2+} + CB7 = CB7\cdot DQ^{2+}$	$PQ^{2+} + CB7 = CB7\cdot PQ^{2+}$
$K = 350\ M^{-1}$	$K = 1.2 \times 10^5\ M^{-1}$
$k_{in} = 1 \times 10^9\ M^{-1}\,s^{-1}$	$k_{in} = 1 \times 10^9\ M^{-1}\,s^{-1}$
$D_{CB7\cdot DQ^{2+}} = 3.0 \times 10^{-6}\ cm^2\,s$	$D_{CB7\cdot PQ^{2+}} = 2.6 \times 10^{-6}\ cm^2\,s$
$DQ^{\bullet+} + CB7 = CB7\cdot DQ^{\bullet+}$	$PQ^{\bullet+} + CB7 = CB7\cdot PQ^{\bullet+}$
$K_r = 1 \times 10^4\ M^{-1}$	$K_r = 6.1 \times 10^4\ M^{-1}$
$k_{r,in} = 1 \times 10^9\ M^{-1}\,s^{-1}$	$k_{r,in} = 1 \times 10^9\ M^{-1}\,s^{-1}$
$D_{CB7\cdot DQ^+} = 3.0 \times 10^{-6}\ cm^2\,s$	$D_{CB7\cdot PQ^+} = 2.6 \times 10^{-6}\ cm^2\,s$
–	$CB7\cdot PQ^{2+} + e^- = CB7\cdot PQ^{\bullet+}$
	$E_{c,1/2} = -0.670\ V$
	$k_c^o = 0.1\ cm/s\ (\alpha = 0.5)$
	$D_{CB7\cdot PQ^{2+}} = D_{CB7\cdot DQ^+} = 2.6 \times 10^{-6}\ cm^2\,s$

very good agreement achieved between the simulated and experimental current–potential curves for both guests at various host concentrations. As mentioned before, one-electron reduction of diquat leads to an increase in the stability of its inclusion complex with CB7 ($K_r = 1 \times 10^4\ M^{-1}$ and $K = 340\ M^{-1}$), while the opposite is true for paraquat ($K_r = 6.1 \times$
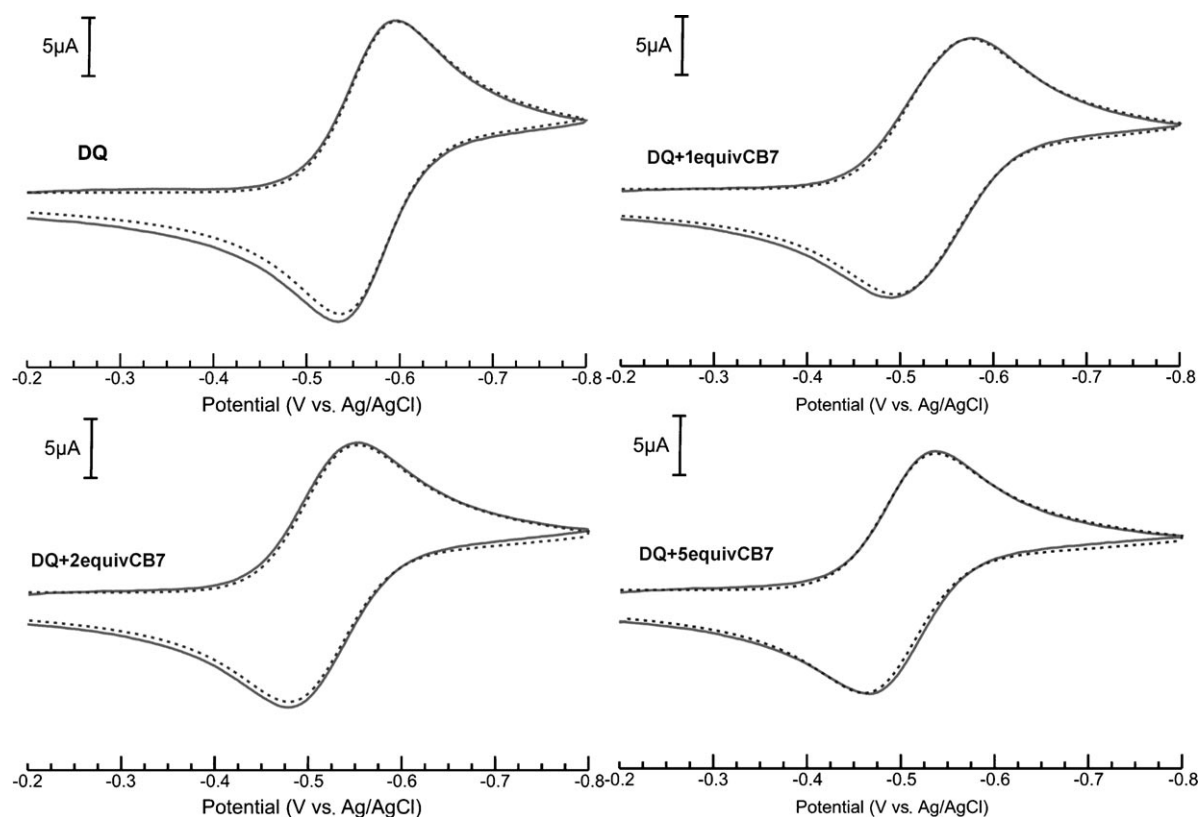

Figure 4. Simulated (dashed) and experimental (solid curves) cyclic voltammograms for DQ^{2+} in the presence of various amounts of CB7. Medium: 0.1 M Phosphate buffer (pH 7). Scan rate: 0.1 V s^{-1}. Background currents subtracted before fitting to the simulations.
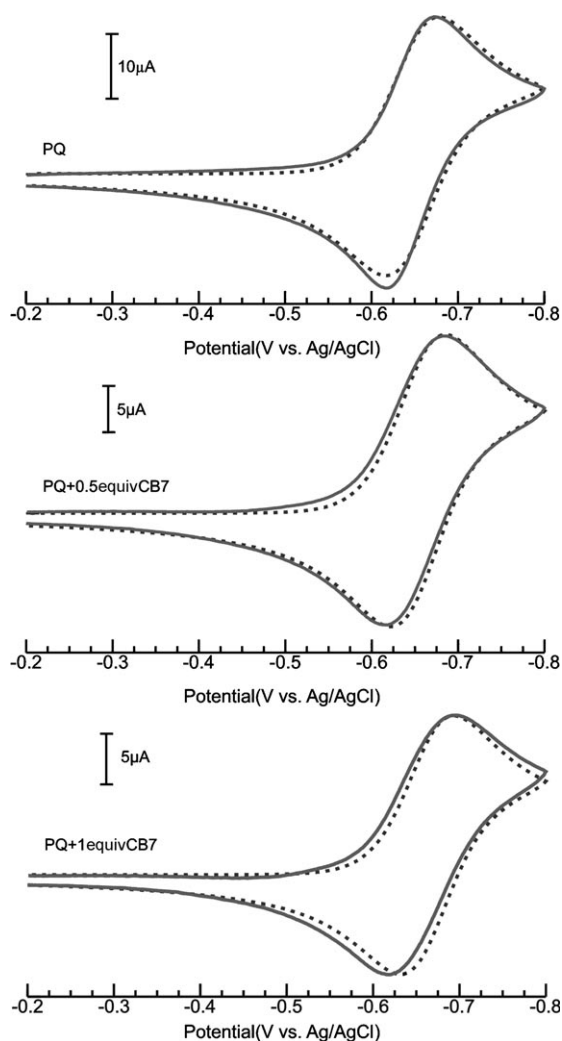
Figure 5. Simulated (dashed) and experimental (solid curves) cyclic voltammograms for PQ^{2+} in the presence of various amounts of CB7. Medium: 0.1 M Phosphate buffer (pH 7). Scan rate: 0.1 V s^{-1}. Background currents subtracted before fitting to the simulations.

10^4 M^{-1} and $K = 1.2 \times 10^5$ M^{-1}). The higher stability of the CB7·PQ^{2+} complex reflects the nice complementarity between the guest and the host. Inclusion of PQ^{2+} by CB7 gives rise to strong ion–dipole interactions between the positively charged nitrogen atoms on the guest and the carbonyl portals on the host in addition to favorable hydrophobic interactions between the aromatic mid-section of the guest and the host cavity. DQ^{2+} exhibits a completely different charge distribution, which fails to fit that on the host, leading to a much weaker complex. Surface electrostatic plots for both guests are shown in the Supporting Information to illustrate this point clearly. One-electron reduction of PQ^{2+} decreases its overall positive charge, but maintains the charge distribution over the structure of the guest, leading to a moderate decrease in its binding affinity with CB7. In the case of DQ^{2+} the positive charges are not ideally located to develop favorable ion–dipole interactions with the carbonyl oxygen atoms on the host portals. Therefore, the ion–

dipole interactions are rather weak, and one-electron reduction decreases the hydrophilic character of the guest, thus increasing the overall stability of the complex.

The binding interactions between the larger cavity host CB8 and DQ^{2+} were also investigated by ^{1}H NMR spectroscopy (Figure 6). All the proton signals of DQ^{2+} gradually
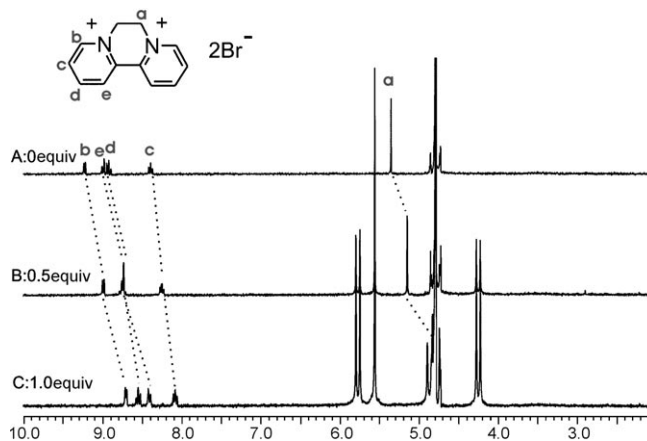

Figure 6. ^{1}H NMR spectra (300 MHz, D$_2$O) of A) 1.0 mM DQ^{2+} in the absence and in the presence of B) 0.5 equiv and C) 1.0 equiv of CB8.

shift upfield in the presence of increasing CB8 concentrations. This includes the signal corresponding to the ethylene bridge, which was unaffected in the presence of CB7. The CB8-induced shifts are pronounced, approximately 0.5–0.6 ppm after addition of one equivalent of host. Furthermore, the observation of a single set of resonances in the surveyed range of CB8 concentrations reveals that the exchange between the free and bound guest is fast on the NMR timescale. In MALDI-TOF mass spectrometric experiments we detected a peak corresponding to the one-electron reduced CB8·DQ^+ complex (see the Supporting Information), which also supports the formation of a 1:1 host–guest complex.

The electronic absorption spectrum of diquat is also affected by the presence of CB8. The molar absorptivity coefficient of DQ^{2+} decreases after addition of increasing concentrations of the host, and the decreasing absorbance values can be analyzed as a function of CB8 concentrations by using a 1:1 binding isotherm to yield a K value of $4.5 \pm 0.6 \times 10^4$ M^{-1} (see data in the Supporting Information). Since this binding constant was determined from relatively small variations in the absorbance values, we also investigated the CB8 effect on the fluorescence emission spectrum of diquat. In contrast to CB7, increasing concentrations of CB8 tend to quench the fluorescence emission of diquat, while the wavelength of maximum emission remains unchanged. This variation of the fluorescence intensity is unusual, as the inclusion of fluorophores inside cucurbit[n]uril hosts typically leads to increased fluorescence emission intensities.[18–20] The origin of this unusual finding may be related to co-inclusion of water, which may facilitate quenching. In any instance, the CB8-induced variation of the fluorescence intensity can
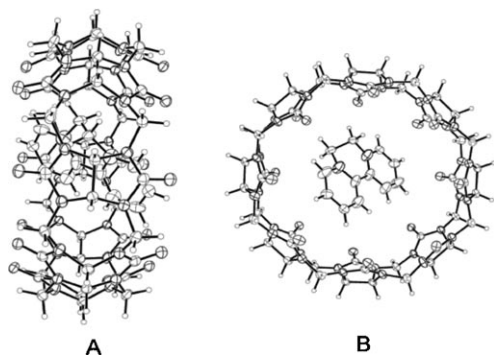
FULL PAPER

Figure 7. Side (left) and top (right) views of the structure of complex $CB8 \cdot DQ^{2+}$ obtained by single-crystal X-ray diffraction methods.
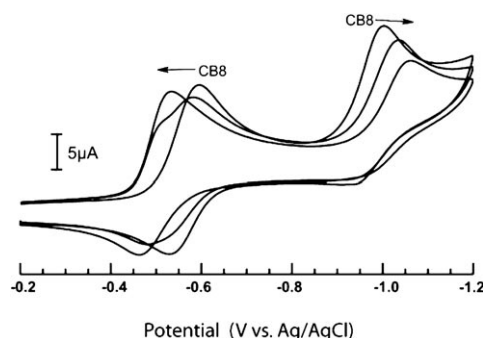

Figure 8. Cyclic voltammetric response of solutions containing 0.57 mM DQ^{2+} in the absence and in the presence of 0.42 and 0.91 equivalents of CB8. Medium: pH 7 0.1 M phosphate buffer. Scan rate: $0.1\,V\,s^{-1}$.

be readily fitted to a 1:1 binding isotherm to yield a K value of $4.8 \pm 0.5 \times 10^4\,M^{-1}$, in very good agreement with the value obtained using electronic absorption data.

The crystallization of CB7 complexes is notoriously difficult, but single crystals of CB8 complexes are easier to prepare. We successfully prepared single crystals of the $CB8 \cdot DQ^{2+}$ complex by slow solvent evaporation of an aqueous solution of the complex. The crystal structure obtained from X-ray diffraction experiments is shown in Figure 7. The guest is clearly included in the cavity of the CB8 host, as shown in the two views of the figure, with the two positively charged nitrogen atoms located inside the cavity. The guest is disordered across a center of symmetry (located at the midpoint of the ethylene bridge C−C bond), such that the atoms in the six-membered aromatic rings coincide in the two orientations, but the two connecting methylene groups do not. The bromide counterions were also severely disordered and a large number of disordered water molecules were also contained in the crystal lattice, thus limiting the final level of structural refinement that could be attained ($R \approx 9\%$). The sample and crystal data for $CB8 \cdot DQ^{2+}$ are summarized in Table SI1 in the Supporting Information. The crystal structure shows that CB8 can include the DQ^{2+} guest without any significant distortion, with the host maintaining its overall D_{8h} symmetry, in contrast with the inclusion complex formed between CB8 and 2,7-dimethyldiazapyrenium,[20] previously crystallized and described by our group, in which the CB8 host shows an elliptical distortion of its cavity.

Cyclic voltammetric experiments can also be utilized to investigate the interactions between DQ^{2+} and CB8. Addition of CB8 to a 1.0 mM solution of DQ^{2+} in phosphate buffer causes significant shifts in the half-wave potentials for its two one-electron reduction processes ($DQ^{2+}/DQ^{\bullet+}$ and $DQ^{\bullet+}/DQ$). Figure 8 details the CB8-induced changes in the voltammetric behavior. The set of waves corresponding to the first reduction process moves to less negative potential, revealing the more pronounced differential stabilization of the reduced form ($DQ^{\bullet+}$). The half-wave potential of the second reduction process ($DQ^{\bullet+}/DQ$) shifts to more negative values, confirming that the monoradical cation is the preferred form for binding inside the CB8 cavity.

This voltammetric behavior raises the possibility that the monoradical cation might dimerize inside the CB8 cavity, in analogy to the behavior observed with the paraquat radical cation.[7] However, the diquat radical cation has been found to be much less prone to dimerization than the corresponding paraquat radical cation,[34,35] which is probably a reflection of the more planar structure of the latter species. We exhaustively reduced solutions of diquat in the absence and in the presence of CB8 and compared the corresponding electronic absorption spectra, but did not detect any significant differences in the energies or intensities of the absorption bands for the reduced species. Therefore, we must conclude that CB8 selectively binds $DQ^{\bullet+}$ in preference to DQ^{2+} or DQ, but we did not obtain any experimental evidence indicating the formation of $CB8 \cdot (DQ^{\bullet+})_2$.

Unfortunately, the very limited solubility of CB8 prevented us from investigating solutions containing $[CB8]/[DQ^{2+}] > 1.0$. This solubility problem made it impossible for us to analyze the current–potential curves by using digital simulations and determine the equilibrium association constant between CB8 and $DQ^{\bullet+}$. We can estimate an approximate value for the corresponding K value of $6 \times 10^5\,M^{-1}$ based on the $E_{1/2}$ shift observed for the $DQ^{2+}/DQ^{\bullet+}$ couple in the presence of about one equivalent CB8 and the measured K value for the $CB8 \cdot DQ^{2+}$ complex.[23]

The contrast between DQ^{2+} and PQ^{2+} regarding their interactions with CB8 is also quite pronounced. As mentioned before, PQ^{2+} forms a stable 1:1 inclusion complex with CB8.[7] One-electron reduction of the guest to its radical cation $PQ^{\bullet+}$ results in the extensive formation of radical cation dimers, stabilized by inclusion complexation inside CB8.[7] In electrochemical terms, the potential window in which $PQ^{\bullet+}$ is stable, against PQ^{2+} and PQ, is substantially widened by addition of CB8. Both PQ^{2+} and $(PQ^{\bullet+})_2$ form stable complexes inside CB8. CB8 has similar phenomenological effects on the electrochemical behavior of DQ^{2+}, but we did not find any spectroscopic evidence for the formation of radical cation dimers $(DQ^{\bullet+})_2$, either free or bound inside CB8. However, one-electron reduction of DQ^{2+} in the presence of CB8 leads to an inclusion complex, $CB8 \cdot DQ^{\bullet+}$ in all likelihood, which is more stable that the original $CB8 \cdot DQ^{2+}$. This contrast probably reflects the con-

siderable differences in charge distribution and, to a lower degree also shape, between paraquat and diquat.

Conclusion

The binding interactions between the guests diquat and paraquat with the hosts CB7 and CB8 span a relatively wide range of binding affinities. From the very stable complex formed between CB7 and PQ^{2+} to the very weak complex between DQ^{2+} and CB7, these interactions reveal that binding of a guest to either host is optimum when the guest has a hydrophobic core that fits well inside the host cavity and a distribution of positive charges that allows the favorable development of ion–dipole interactions between the charges on the guest and the oxygen-laced portals of the host. This explains the already reported stability of the $CB7 \cdot PQ^{2+}$ and $CB8 \cdot (PQ^{\bullet+})_2$ complexes. The two positive charges on diquat are not well positioned for development of ion–dipole interactions with the portals of CB7 and make the core of the guest too hydrophilic for inclusion inside the host cavity. Therefore, DQ^{2+} is only weakly bound by CB7. One-electron reduction, however, improves the stability of its CB7 complex, as opposed to what is observed with the $PQ^{2+}/PQ^{\bullet+}$ couple. An interesting finding of this work is that CB8 appears to tolerate better the charge distribution present in DQ^{2+}, and both DQ^{2+} and its one-electron reduced form are both bound with reasonable affinity ($K > 10^4 \, \text{M}^{-1}$) inside this host.

Experimental Section

Materials and procedures: Diquat,[36] CB7 and CB8[37] were prepared following literature procedures. All other materials were commercially available and used as received. Water was purified in a Barnstead Nanopure II four-cartridge system to a resistivity better than $18 \, \text{m}\Omega \, \text{cm}^{-1}$. The voltammetric experiments were performed with a Bioanalytical Systems 100B/W electrochemical workstation. The experiments were carried out in a single compartment cell fitted with a glassy carbon working electrode ($0.071 \, \text{cm}^2$), a platinum wire counter electrode, and a Ag/AgCl reference electrode. The working electrode was polished with $0.05 \, \mu\text{m}$ alumina/water slurry on a felt surface. The solutions were purged with purified nitrogen gas and kept under an inert nitrogen atmosphere during the electrochemical experiments.

X-ray diffraction experiments: All experimental, data collection and analysis details are described in the Supporting Information. CCDC-639751 contains the supplementary crystallographic data for this paper. These data can be obtained free of charge from The Cambridge Crystallographic Data Centre via www.ccdc.cam.ac.uk/data_request/cif.

Acknowledgements

[1] P. Monk, *The Viologens: Physicochemical Properties, Synthesis and Applications of the Salts of 4,4'-Bipyridine*, Wiley, New York, **1998**, Chapter 5.

[2] J. W. Lee, S. Samal, N. Selvapalam, H.-J. Kim, K. Kim, *Acc. Chem. Res.* **2003**, *36*, 621.

[3] J. Lagona, P. Mukhopadhyay, S. Chakrabarti, L. Isaacs, *Angew. Chem.* **2005**, *117*, 4922; *Angew. Chem. Int. Ed.* **2005**, *44*, 4844.

[4] J. Kim, I.-S. Jung, S.-Y. Kim, E. Lee, J.-K. Kang, S. Sakamoto, K. Yamaguchi, K. Kim. , *J. Am. Chem. Soc.* **2000**, *122*, 540.

[5] H.-J. Kim, W. S. Jeon, Y. H. Ko, K. Kim, *Proc. Natl. Acad. Sci. USA* **2002**, *99*, 5007.

[6] W. Ong, M. Gomez-Kaifer, A. E. Kaifer, *Org. Lett.* **2002**, *4*, 1791.

[7] Y. J. Jeon, H.-J. Kim, C. Lee, K. Kim. *Chem. Commun.* **2002**, 1828.

[8] H.-J. Kim, J. Heo, W. S. Jeon, E. Lee, J. Kim, S. Sakamoto, K. Yamaguchi, K. Kim, *Angew. Chem.* **2001**, *113*, 1574; *Angew. Chem. Int. Ed.* **2001**, *40*, 1526.

[9] W. S. Jeon, P. K. Bharadwaj, S. W. Choi, J. W. Lee, K. Kim, *Angew. Chem.* **2002**, *114*, 4654; *Angew. Chem. Int. Ed.* **2002**, *41*, 4474.

[10] J. W. Lee, K. Kim, S. W. Choi, Y. H. Ko, S. Sakamoto, K. Yamaguchi, K. Kim, *Chem. Commun.* **2002**, 2692.

[11] W. S. Jeon, A. Y. Ziganshina, Y. H. Ko, J.-K. Kang, J. W. Lee, C. Lee, K. Kim, *Angew. Chem.* **2003**, *115*, 4231; *Angew. Chem. Int. Ed.* **2003**, *42*, 4097.

[12] K. Kim, D. Kim, J. W. Lee, Y. H. Ko, K. Kim, *Chem. Commun.* **2004**, 848.

[13] Y. H. Ko, K. Kim, J.-K. Kang, H. Chun, J. W. Lee, S. Sakamoto, K. Yamaguchi, J. C. Fettinger, K. Kim, *J. Am. Chem. Soc.* **2004**, *126*, 1932.

[14] W. S. Jeon, E. Kim, Y. H. Ko, I. Hwang, J. W. Lee, S.-Y. Kim, H.-J. Kim, K. Kim, *Angew. Chem.* **2005**, *117*, 89; *Angew. Chem. Int. Ed.* **2005**, *44*, 87.

[15] Y. H. Ko, Eunju Kim, I. Hwang, K. Kim, *Chem. Commun.* **2007**, 1305.

[16] K. Moon, J. Grindstaff, D. Sobransingh, A. E. Kaifer, *Angew. Chem.* **2004**, *116*, 5612; *Angew. Chem. Int. Ed.* **2004**, *43*, 5496.

[17] W. Wang, A. E. Kaifer, *Angew. Chem.* **2006**, *118*, 7200; *Angew. Chem. Int. Ed.* **2006**, *45*, 7042.

[18] V. Sindelar, M. A. Cejas, F. M. Raymo, A. E. Kaifer, *New J. Chem.* **2005**, *29*, 280.

[19] Y. Ling, W. Wang, A. E. Kaifer, *Chem. Commun.* **2007**, 610.

[20] V. Sindelar, M. A. Cejas, F. M. Raymo, W. Chen, S. E. Parker, A. E. Kaifer, *Chem. Eur. J.* **2005**, *11*, 7054.

[21] See, for instance: W. Ong, A. E. Kaifer, *J. Org. Chem.* **2004**, *69*, 1383.

[22] T. Pérez-Ruiz, C. Martínez-Lozano, V. Tomás, J. Fenoll, *Analyst* **2000**, *125*, 2372.

[23] A. E. Kaifer, M. Gómez-Kaifer, *Supramolecular Electrochemistry*, Wiley-VCH, Weinheim, **1999**, Chapter 9.

[24] The program used for digital simulations was DigiElch v2.0. The program was used under permission from ElchSoft. References [25–29] provide theoretical background for the simulation program.

[25] M. Rudolph, *J. Electroanal. Chem.* **2003**, *543*, 23.

[26] M. Rudolph, *J. Electroanal. Chem.* **2004**, *571*, 289.

[27] M. Rudolph, *J. Comput. Chem.* **2005**, *26*, 619.

[28] M. Rudolph, *J. Comput. Chem.* **2005**, *26*, 633.

[29] M. Rudolph, *J. Comput. Chem.* **2005**, *26*, 1193.

[30] T. Matsue, D. H. Evans, T. Osa, N. Kobayashi, *J. Am. Chem. Soc.* **1985**, *107*, 3411.

[31] R. Isnin, C. Salam, A. E. Kaifer, *J. Org. Chem.* **1991**, *56*, 35.

[32] Y. Wang, S. Mendoza, A. E. Kaifer, *Inorg. Chem.* **1998**, *37*, 317.

[33] Y. Cohen, L. Avram, L. Frish, *Angew. Chem.* **2005**, *117*, 524; *Angew. Chem. Int. Ed.* **2005**, *44*, 520.

[34] P. S. Braterman, J.-I. Song, *J. Org. Chem.* **1991**, *56*, 4678.

[35] E. F. Bowden, F. M. Hawkridge, *J. Electroanal. Chem. Interfacial Electrochem.* **1981**, *125*, 367.

[36] J. E. Dickeson, L. A. Summers, *Experientia* **1969**, *25*, 1274.

[37] A. Day, A. P. Arnold, R. J. Blanch, B. Snushall, *J. Org. Chem.* **2001**, *66*, 8094.